J Mater Sci (2009) 44:4315–4320
DOI 10.1007/s10853-009-3641-2

Effect of heat-treatment on CdS and CdS/ZnS nanoparticles

Kwanhwi Park · Hong Jeong Yu · Won Keun Chung · Byung-Jea Kim · Sung Hyun Kim

Received: 25 February 2009 / Accepted: 23 May 2009 / Published online: 18 June 2009

Abstract Mono-dispersed and spherical cadmium sulfide (CdS) nanoparticles and cadmium sulfide/zinc sulfide (CdS/ZnS) nanoparticles, 4–5 nm in diameter, were synthesized in a heptane-AOT-water microemulsion system. The heat treatment of CdS and CdS/ZnS nanoparticles was annealed at 570 °C under the air atmosphere. The heat-treated nanoparticles were of variable large sizes and had enhanced crystallinity. UV–Vis spectra of heat-treated CdS and CdS/ZnS nanoparticles revealed a flat shape similar to that of bulk CdS compounds. The difference between the PL emission bands of organic-coated nanoparticles and heat-treated nanoparticles was small. The PL emission energy of heat-treated nanoparticles was improved by about 2–3 times compared with that of organic-coated nanoparticles.

Introduction

Nanometer-sized inorganic semiconductor compounds have attracted considerable attention due to their novel size-dependent characteristics [1–3] and different physico-chemical and optoelectronic properties compared with the corresponding bulk compounds. The synthesis methods for the nanometer-sized inorganic semiconductor have been studied, and applications have been developed in which to utilize the novel physical and chemical properties of nanometer-sized semiconductors, such as photovoltaic and light emitting devices [4–7].

The band gap of II–VI semiconductor nanoparticles such as CdSe [8, 9], CdS [10–13], and ZnS [14] can be varied by quantum effects that depend on the sizes of II–VI semiconductor nanoparticles. Many techniques, such as microemulsion methods and chemical vapor deposition, have been developed to synthesize mono-dispersed II–VI semiconductor nanoparticles. The microemulsion synthesis methods for nanoparticles were previously reported in several studies [9–11, 15]. In the microemulsion system, changing the reaction conditions such as the concentration of precursors and the ratio of water to surfactant allows easy control of the size and distribution of the colloidal crystallites [16].

There are several methods, such as luminescent ion doping, optical annealing, and shell compound coating, that are effected to increase the luminescence of II–VI semiconductor nanoparticles. Doping of luminescent ions into semiconductor materials is one method to obtain a desired emission wavelength. In nanoparticles doped with luminescent ions, efficient energy transfer occurs from host to luminescent ions [17]. Tm- and Li-codoped, Mn-doped, and Sm-doped ZnS semiconductors emit blue, orange, and red light, respectively [18–20]. Optical annealing reduces the severe non-radiative recombination due to polymerization and photo-oxidation and enhances the crystal quality of the nanoparticles [21, 22]. Core/shell-type nanoparticles over-coated with higher band-gap inorganic materials exhibit high PL quantum yield compared with uncoated dots, due to elimination of surface non-radiative recombination defects. The improvement of emission energy in core/shell structures such as CdSe/CdS [23, 24] and CdSe/ZnS [25] have previously been reported in several studies. However, heat treatment of II–VI group semiconductor nanoparticles synthesized microemulsion method was not

K. Park · H. J. Yu · W. K. Chung · B.-J. Kim · S. H. Kim (✉)
Department of Chemical & Biological Engineering, Korea University, 1,5-Ka, Anam-Dong, Sungbuk-Ku, Seoul 136-701, Republic of Korea
e-mail: kimsh@korea.ac.kr

investigated as an enhancer of luminescent properties. Heat treatment is a reasonable method to enhance the luminescent properties through removal of organic or surface oxidation particles, etc. This study was designed to investigate the effect of heat treatment on CdS nanoparticles and CdS/ZnS nanoparticles that were synthesized by a general microemulsion method.

Mono-dispersed and spherical cadmium sulfide (CdS) and cadmium sulfide/zinc sulfide (CdS/ZnS) nanoparticles, 4–5 nm in diameter, were synthesized from aqueous cadmium acetate dehydrate, zinc acetate dehydrate, and sodium sulfide nonahydrate. The effect of heat treatment on CdS nanoparticles and CdS/ZnS nanoparticles was investigated and the changes in the properties of CdS nanoparticles and CdS/ZnS nanoparticles following heat treatment were characterized.

Experiments

To synthesize CdS nanoparticles, 10 mL of aqueous 0.01 M cadmium acetate dehydrate [$Cd(CH_3COO)_2 \cdot 2H_2O$] solution and 100 mL of 0.1 M AOT (dioctyl sulfosuccinate sodium salt) in heptane were mixed for 1 h. Dodecanethiol (0.25 mL) was added and mixed for 30 min. Ten milliliters of aqueous 0.01 M sodium sulfide nonahydrate ($Na_2S \cdot 9H_2O$) solution was added slowly and the microemulsion solution was stirred for 1 h to complete the reaction. The solvent was removed using a rotary evaporator. The resulting sample was rinsed in ethanol to precipitate the nanoparticles and to remove the adsorbed AOT, thiol, and byproducts. After filtering through filter paper, the nanoparticles were dispersed in ethanol and THF. To synthesize CdS/ZnS nanoparticles, 10 mL of aqueous 0.01 M zinc acetate dehydrate [$Zn(CH_3COO)_2 \cdot 2H_2O$] solution was added to the CdS nanoparticles solution, which was synthesized with Cd and S precursors as explained above; the microemulsion solution was then mixed for 30 min. Ten milliliters of aqueous 0.01 M $Na_2S \cdot 9H_2O$ solution was added slowly and stirred for 1 h. After purification by evaporation and filtering, the nanoparticles were dispersed in ethanol and THF.

Heat treatment of CdS nanoparticles and CdS/ZnS nanoparticles was performed in air. The CdS nanoparticles and CdS/ZnS nanoparticles were heat treated at 570 °C for 2 h to remove organic materials. The heat-treated nanoparticles were then cooled to room temperature and dispersed in ethanol or THF. The CdS nanoparticles and CdS/ZnS nanoparticles were analyzed by Fourier transform infrared spectroscopy (FT-IR), thermo-gravimetric analysis (TGA), transmission electron microscopy (TEM), X-ray diffraction (XRD), ultraviolet/visible light (UV–Vis) spectroscopy, and photo-luminescence (PL).

Results and discussion

Figure 1 shows the FT-IR spectra of the CdS nanoparticles (a), CdS/ZnS nanoparticles (b), heat-treated CdS nanoparticles (c), heat-treated CdS/ZnS nanoparticles (d), and pure AOT (e). The FT-IR bands for related Cd^{2+} and Zn^{2+} compounds are listed in Table 1. In Fig. 1, the FT-IR bands of CdS nanoparticles (a) and CdS/ZnS nanoparticles (b) consist of CdS (620, 1120, and 3440 cm^{-1}), ZnS (680, 1120, and 3440 cm^{-1}), and AOT (1400–1500 and 2800–2900 cm^{-1}). The FT-IR bands indicate that AOT-capped CdS nanoparticles and CdS/ZnS nanoparticles were successfully synthesized. In the FT-IR of heat-treated CdS nanoparticles (c) and CdS/ZnS nanoparticles (d), the bands related to AOT (2800–2900 cm^{-1}) are smaller than those in (a) and (b) due to the removal of organic materials by heat treatment. The sulfate compound bands (600–650 and 1100–1200 cm^{-1}) are larger than those before heat treatment because of the formation of sulfate compounds like $CdSO_4$ and $ZnSO_4$ by oxidation at high temperature in air.

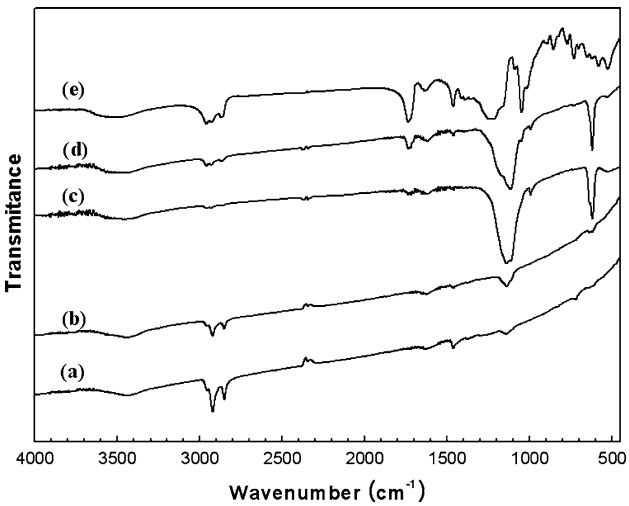

Fig. 1 FT-IR spectra of CdS nanoparticles (*a*), CdS/ZnS nanoparticles (*b*), heat-treated CdS nanoparticles (*c*), heat-treated CdS/ZnS nanoparticles (*d*), and pure AOT (*e*)

Table 1 FT-IR bands for related Cd^{2+} and Zn^{2+} compounds

Compound		Band position (cm^{-1})
Sulfide compound	CdS	620, 1120, 1610, 3440
	ZnS	630, 1110, 1620, 3440
Sulfate compound	$CdSO_4$	585, 620, 680, 990, 1120, 1610, 1740
	$ZnSO_4$	630, 735, 1100, 1150, 1630, 2210
Oxide compound	CdO	725
	ZnO	725, 1350

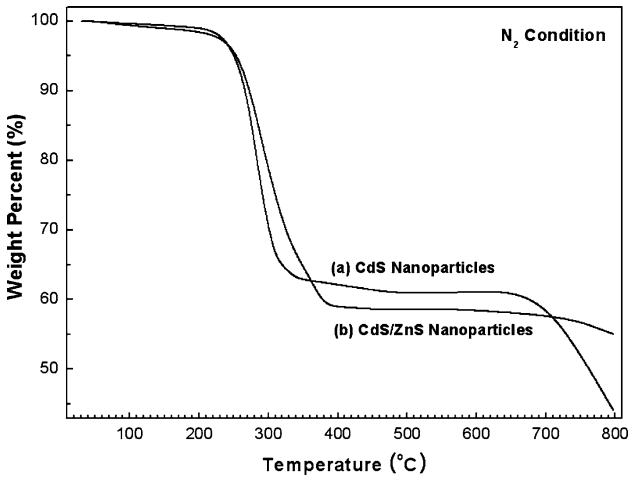

Fig. 2 TGA graph of CdS nanoparticles (*a*) and CdS/ZnS nanoparticles (*b*) under nitrogen condition (heating rate: 10 °C/min)

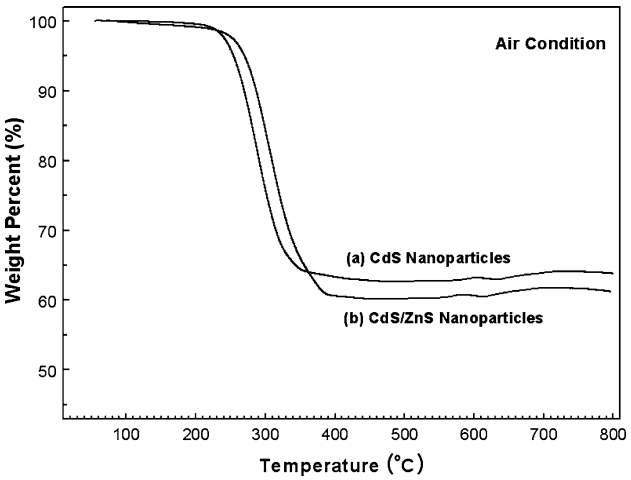

Fig. 3 TGA graph of CdS nanoparticles (*a*) and CdS/ZnS nanoparticles (*b*) under air condition (heating rate: 10 °C/min)

Figure 2 shows the TGA graphs for CdS nanoparticles (a) and CdS/ZnS nanoparticles (b) analyzed under nitrogen atmosphere condition. The heating rate for TGA was 10 °C/min. The TGA graphs for both CdS and CdS/ZnS nanoparticles in Fig. 2 consist of two weight reduction sections. The first weight reduction from 220 to 380 °C is due to removal of organic materials. These results correspond with the decrease in bands related to AOT (2800–2900 cm^{-1}) in the heat-treated nanoparticles in Fig. 1. The inorganic weight portions of the CdS nanoparticles and CdS/ZnS nanoparticles, as estimated from the TGA graph in Fig. 2, are 61 and 58%, respectively. The second weight reduction above 650 °C may be the effect of inorganic compound sublimation. Because the intermolecular force of the nanoparticles was weaker than that of the bulk compounds, the CdS nanoparticles and CdS/ZnS nanoparticles sublimated at lower temperature than the bulk CdS (900 °C) and ZnS (1,185 °C) under nitrogen. The weight reduction rate of CdS/ZnS nanoparticles was slower than that of CdS nanoparticles because ZnS has a higher sublimation point than CdS. Figure 3 shows the TGA graphs for the CdS nanoparticles (a) and the CdS/ZnS nanoparticles (b) analyzed under air atmosphere condition. The TGA graphs for both CdS and CdS/ZnS nanoparticles in Fig. 3 consist one weight reduction section without weight reduction above 650 °C. The weight reduction from 220 to 380 °C is due to removal of organic materials like Fig. 2. The inorganic weight portions of the CdS and CdS/ZnS nanoparticles heat treated under air, as estimated from the TGA graph in Fig. 3, are 64 and 61%, respectively. The inorganic weight portions of the heat-treated nanoparticles under air is little higher than ones under nitrogen due to the formation of the sulfate under air. The most important discrepancy between TGA graph of nanoparticles analyzed under nitrogen and air atmosphere condition is that absence of weight reduction by sublimation above 650 °C. This phenomenon is the effect of the formation of the sulfate by reaction between sulfur in nanoparticles and oxygen in air.

Figure 4 shows the TEM images of CdS nanoparticles (a), CdS/ZnS nanoparticles (b), heat-treated CdS nanoparticles (c), and heat-treated CdS/ZnS nanoparticles (d). The TEM samples were prepared by drying carbon-coated copper grid dipped in nanoparticles dispersed in ethanol. Figure 4a and b confirms that mono-dispersed and almost spherical CdS nanoparticles and CdS/ZnS nanoparticles, 4–5 nm in diameter, were synthesized. This result indicates that the ZnS layer coated on the CdS core is very thin. The thin ZnS layer corresponds to values calculated from physical properties of the products such as density, molecular weight, etc. These images also show that the CdS and CdS/ZnS nanoparticles maintain their size without aggregation. However, the nanoparticles also appear to contain trapped solvent such as heptane in Fig. 4a and b. The heat-treated CdS and CdS/ZnS nanoparticles have variable shapes and sizes, from a few tens to hundreds of nanometers with aggregation and the trapped solvent disappeared as shown in Fig. 4c and d.

Figure 5 shows the XRD patterns of the CdS nanoparticles (a) and CdS/ZnS nanoparticles (b). The diffraction pattern of the CdS nanoparticles shows three structured peaks at 25–30°, 42–45°, and 50–55°. The broadening of the diffraction peaks is due to the finite size of the nanoparticles. The peak at 25–30° might be due to the convolution of the three peaks corresponding to (100), (002), and (101) of the hexagonal CdS phase, as shown by the vertical bar of CdS in Fig. 5. The peak of 42–45° is effect of (110) peak of the hexagonal CdS phase and the peak of 50–55° is effect of convolution of (200), (112), and (201) peaks. The diffraction pattern of the CdS/ZnS nanoparticles shows two structured peaks at 25–30° and 42–55°. The peak at 25–30°

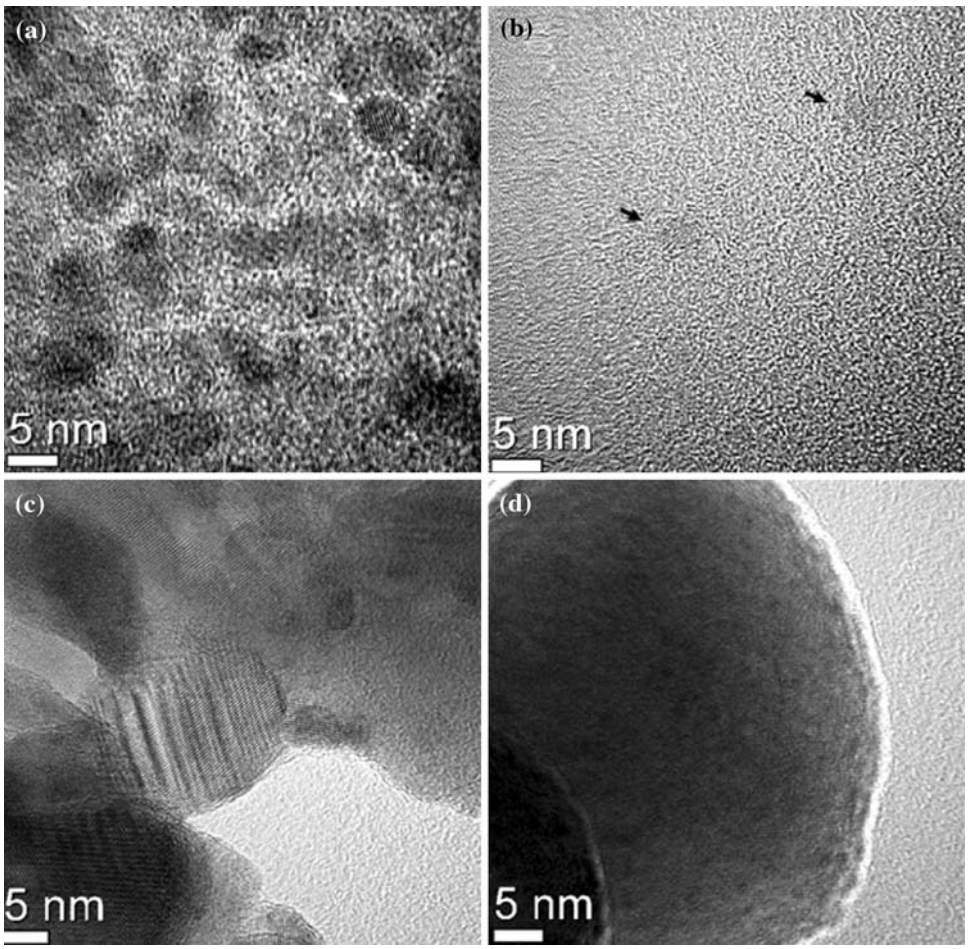

Fig. 4 TEM images of CdS nanoparticles (**a**), CdS/ZnS nanoparticles (**b**), heat-treated CdS nanoparticles (**c**), and heat-treated CdS/ZnS nanoparticles (**d**). All nanoparticles were dispersed in ethanol

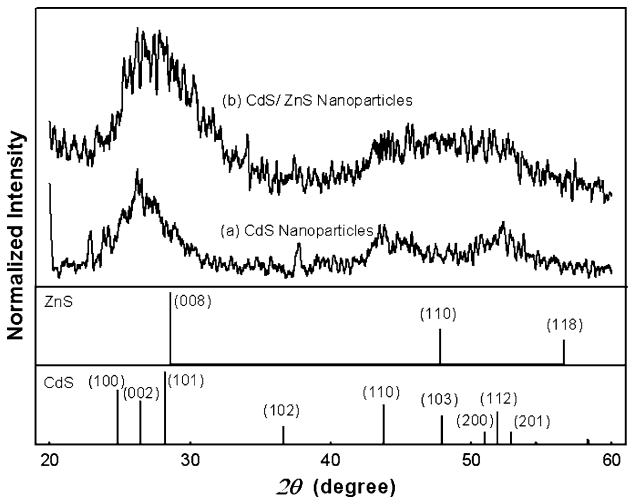

Fig. 5 The XRD patterns of CdS nanoparticles (*a*) and CdS/ZnS nanoparticles (*b*) were synthesized in a heptane-AOT-water microemulsion system (reference: JCPDS 06-0314(CdS) and JCPDS 39-1363(ZnS))

of CdS/ZnS nanoparticles is broader than it of CdS nanoparticles due to the convolution of the peak of the CdS nanoparticles and (008) peak of ZnS. And the flat-type peak at 42–55° might be due to the convolution of the peak at 42–45° and 50–55° of the CdS nanoparticles and (110) peak of ZnS.

Figure 6 shows the XRD patterns of the heat-treated CdS nanoparticles (a) and heat-treated CdS/ZnS nanoparticles (b). The XRD patterns of the heat-treated CdS nanoparticles are much shaper than organic-coated CdS nanoparticles and correspond with the XRD patterns of hexagonal CdS. The shaper XRD patterns mean that the size of the CdS nanoparticles was increased and the crystallinity of the CdS nanoparticles was enhanced by heat treatment like TEM image of the heat-treated CdS nanoparticles in Fig. 4c. The XRD patterns of the heat-treated CdS/ZnS showed same phenomenon with CdS nanoparticles and correspond with XRD patterns of the mixture of hexagonal CdS and ZnS.

Figure 7 shows UV–Vis spectra of CdS nanoparticles (a), CdS/ZnS nanoparticles (b), heat-treated CdS (c), and heat-treated CdS/ZnS nanoparticles (d). In Figure 7a and b, the absorption edge of CdS nanoparticles and CdS/ZnS nanoparticles occurs at ca. 380 nm. In Fig. 4c and d, UV–Vis spectra of heat-treated CdS nanoparticles and CdS/ZnS nanoparticles are a flat type, similar to bulk CdS compounds.

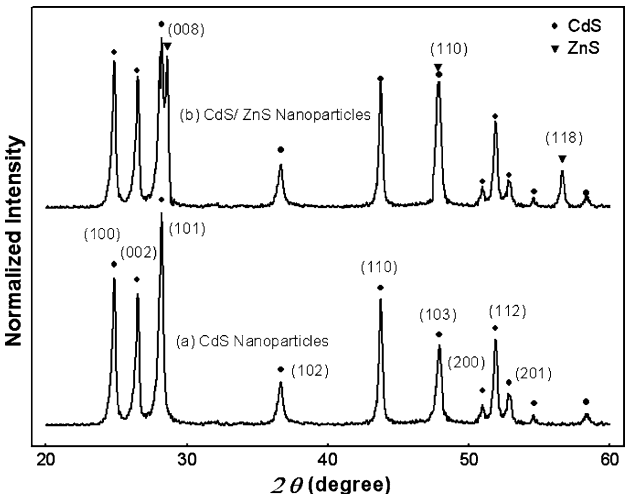

Fig. 6 The XRD patterns of CdS nanoparticles (*a*) and CdS/ZnS nanoparticles (*b*) were heat-treated in air (reference: JCPDS 06-0314(CdS) and JCPDS 39-1363(ZnS))

As a result, it is difficult to define the absorption peak of heat-treated CdS and CdS/ZnS nanoparticles. These results show the effect of heat treatment on particle growth as shown in Fig. 4c and d.

Figure 8 shows the PL spectra of CdS nanoparticles (a), CdS/ZnS nanoparticles (b), heat-treated CdS (c), and heat-treated CdS/ZnS nanoparticles (d) exited by 325 nm He–Cd laser. In the PL spectra of CdS nanoparticles (a), the emission band is seen near 410 nm. The PL emission energy of CdS/ZnS nanoparticles is greater than that of CdS nanoparticles at ca. 410 nm. The PL enhancement of CdS/ZnS nanoparticles is due to passivation, which means that surface atoms are bound to the shell material that has both similar lattice constant and larger band gap [25]. In Fig. 8c and d, the PL emission band of the heat-treated CdS and CdS/ZnS nanoparticles shifted to a wavelength about 20 nm longer than that of the organic-coated CdS and CdS/ZnS nanoparticles due to particle growth following heat treatment. The PL emission energy of the heat-treated CdS nanoparticles improves by about 2 times that of the organic-coated nanoparticles, while the PL emission energy of the heat-treated CdS/ZnS nanoparticles improved by about 3 times. The increases in the PL emission energy of the nanoparticles are due to the enhanced crystallinity and the formation of a sulfate-compound shell following heat treatment. The heat treatment helps improving the crystallinity of nanoparticles as shown in Figs. 4, 5, and 6. Heat treatment in air can also induce the oxidation of nanoparticles.

If the nanoparticle sizes are variable and large, as shown in Fig. 4c and d, it is not possible for the PL spectra of nanoparticles to be narrow with high emission energy as shown in Fig. 8c and d. The luminescent particles of organic-coated nanoparticles and heat-treated nanoparticles are similar because the difference between PL emission bands of organic-coated nanoparticles and ones of the heat-treated nanoparticle is little. Thus, we think that structure of heat-treated nanoparticles is such that luminescent particles, such as CdS and CdS/ZnS nanoparticles, are dispersed homogenously in sulfate compounds.

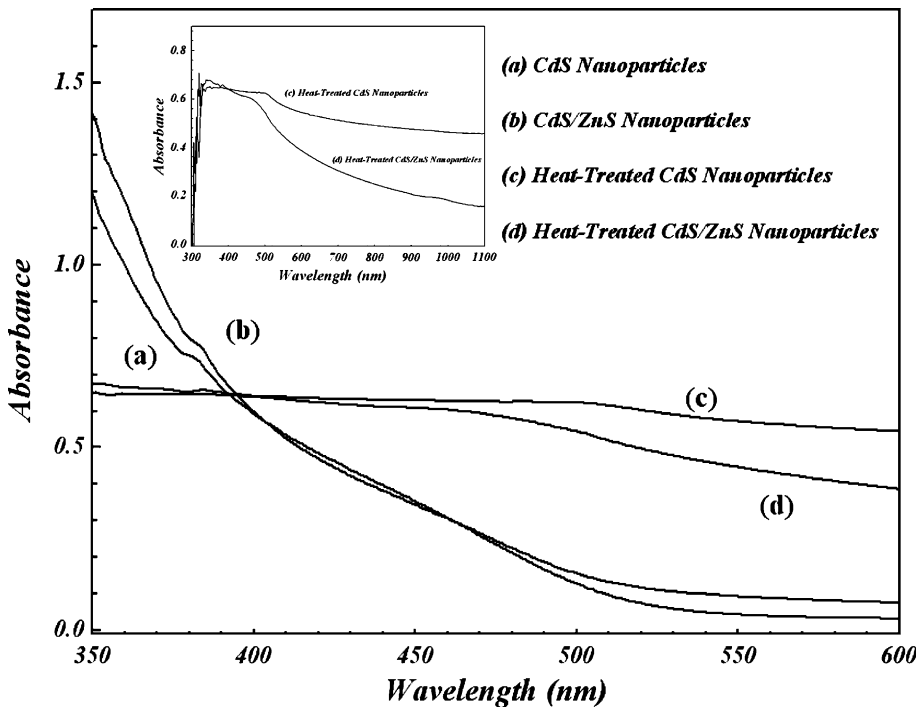

Fig. 7 UV–Vis spectra of CdS nanoparticles (*a*), CdS/ZnS nanoparticles (*b*), heat-treated CdS nanoparticles (*c*), and heat-treated CdS/ZnS nanoparticles (*d*). All nanoparticles were dispersed in THF (*inset*: UV–Vis spectra of heat-treated CdS nanoparticles (*c*), and heat-treated CdS/ZnS nanoparticles over a wide range of wavelengths)

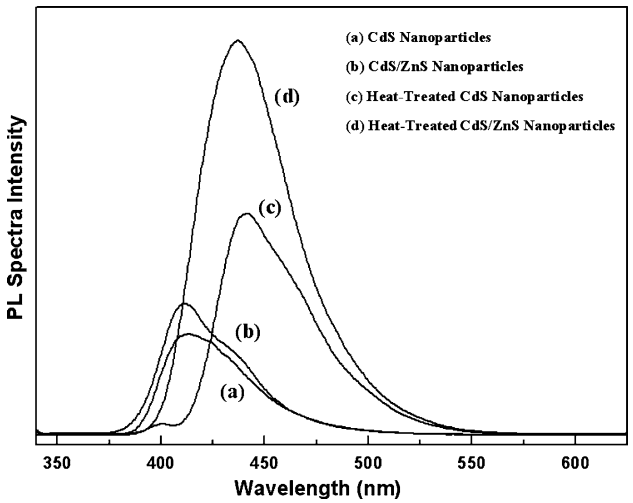

Fig. 8 PL spectra of CdS nanoparticles (*a*), CdS/ZnS nanoparticles (*b*), heat-treated CdS nanoparticles (*c*), and heat-treated CdS/ZnS nanoparticles (*d*). All nanoparticles were dispersed in THF

Conclusion

Mono-dispersed and spherical CdS and CdS/ZnS nanoparticles, 4–5 nm in diameter, were synthesized successfully in a heptane-AOT-water microemulsion system. The effects of heat treatment on the nanoparticles were characterized by FT-IR, TGA, TEM, XRD, UV–Vis absorption, and PL spectra. Sulfate compounds were formed by oxidation at high temperature in air. The UV–Vis spectra of heat-treated CdS and CdS/ZnS nanoparticles reveal a flat type, similar to bulk CdS compounds. The difference between the PL emission bands of organic-coated nanoparticles and heat-treated nanoparticles is small. The PL emission energy of heat-treated nanoparticles improves by 2–3 times compared to that of organic-coated nanoparticles; this increase is due to the enhanced crystallinity and the formation of the sulfate shell.

Acknowledgement The authors are grateful for financial support for this work from the Carbon Dioxide Reduction and Sequestration Center, a 21st Century Frontier R&D Program funded by the Ministry of Science and Technology of Korea.

References

1. Wong EW, Sheehan PE, Lieber CM (1997) Science 277:1971
2. Peng X, Manna L, Yang W, Wickham J, Scher E, Kadavanich A, Alivisatons AP (2000) Nature 404:59
3. Park SJ, Kim S, Lee S, Khim ZG, Char K, Hyeon T (2000) J Am Chem Soc 122:8581
4. Colvin VL, Schlamp MC, Alivisatos AP (1994) Nature 370:354
5. Ahmadi TS, Wang ZL, Green TC, Henglein A, El-Sayed MA (1996) Science 272:1924
6. Mattoussi H, Radzilowski LH, Dabbousi BO (1999) J Appl Phys 86:4390
7. Coe S, Woo WK, Bawendi M, Bulovic V (2002) Nature 420:800
8. Chen X, Nazzal AY, Xiao M, Peng ZA, Peng X (2002) J Lumin 97:205
9. Talapin DV, Poznyak SK, Gaponik NP, Rogach AL, Eychmüller A (2002) Physica E 14:237
10. Qi L, Cölfen H, Antonietti M (2001) Nano Lett 1(2):61
11. Ohde H, Ohde M, Bailey F, Kim H, Wai CM (2002) Nano Lett 2(7):721
12. Zhao FH, Su Q, Xu NS, Ding CR, Wu MM (2006) J Mater Sci 41:1449. doi:10.1007/s10853-006-7459-x
13. Park K, Yu HJ, Kang HU, Kim S, Kim SH (2007) Jpn J Appl Phys 46(10A):6878
14. Valkonen MP, Kanniainen T, Lindroos S, Leskelä M, Rauhala E (1997) Appl Surf Sci 115:386
15. Zhang Y, Wang X, Fu DG, Cheng JQ, Shen YC, Liu JZ, Lu ZH (2001) J Phys Chem Solids 62:903
16. Steigerwald ML, Alivisatos AP, Gibson JM, Harris TD, Kortan R, Muller AJ, Thayer AM, Duncan TM, Douglass DC, Brus LE (1987) J Am Chem Soc 110(10):3046
17. Bhargava RN, Gallagher D (1994) Phys Rev Lett 72:416
18. Zavyalova LV, Savin AK, Svechnikov GS (1997) Displays 18:73
19. Stambouli AB, Hamzaoui S, Bouderbala M (1996) Thin Solid Films 283:204
20. Tang T, Yang M, Chen K (2000) Ceram Int 26:153
21. Stepanov AL, Popok VN (2004) Surf Coat Technol 185:30
22. Choo C, Sakamoto T, Tohara M, Tanaka K, Nakata R, Okuyama N (2000) Surf Sci 445:480
23. Peng XG, Schlamp MC, Kadavanich AV, Alivisatos AP (1997) J Am Chem Soc 119:7019
24. Xu L, Huang X, Zhu J, Chen H, Chen K (2000) J Mater Sci 35:1375. doi:10.1023/A:1004786224687
25. Song KK, Lee S (2000) Curr Appl Phys 1:167